

Recovery of Lattice Parameter and Electrical Resistivity in Low-Temperature Neutron-Irradiated Copper

E. E. Gruber, J. A. Tesk, T. H. Blewitt, and R. E. Black

Materials Science Division, Argonne National Laboratory, Argonne, Illinois 60439

(Received 27 May 1970)

The fast-neutron-irradiation-induced change and subsequent isochronal annealing recovery of the lattice parameter and electrical resistivity of copper were studied. A wire resistivity specimen and single crystal were irradiated together in liquid helium and transferred to a cryostat without warm up. The simultaneous recovery of both properties was measured at 4.2°K following isochronal anneals to temperatures as high as 675°K. The results of the three successful experimental runs were in good agreement. An analysis, based on linear superposition of the effects of the individual defects, is presented as the simplest and most direct approach to determine the migration mechanism as a function of temperature. The most significant and unambiguous conclusion of this analysis is that stage-III recovery in copper (220–280°K) is due to vacancy migration. Alternative explanations in terms of more complex phenomena appear less probable, but cannot be excluded with certainty.

I. INTRODUCTION

The short-range objective of radiation damage studies is to determine specifically the nature and behavior of the radiation-induced defects. Since the defects are generally not directly observable, their characteristics must be determined from measurements of changes in some physical property of the material.

Much of the work that has been done in the field of radiation damage has been concerned with the electrical resistivity change occurring during irradiation or subsequent annealing. Such studies have been carried out with a variety of materials, irradiating species, and experimental conditions.¹ A great advantage of electrical resistivity measurements is the degree of accuracy that can be obtained. Despite the highest accuracy, however, there remains a thriving controversy over the explanation of annealing data in terms of migration of specific defects.²

It is generally agreed that some correlated recombination of interstitials and vacancies takes place at very low temperatures (in stage I), and that interstitials migrate freely at slightly higher temperatures (at the end of stage I, perhaps). The controversial point is whether a second type of interstitial or a vacancy is the migrating species in the stage-III region in copper, from about 220°K to room temperature.

The reason that this controversy is difficult to resolve is that almost all of the recovery occurs by mutual annihilation of vacancies and interstitials, no matter what the migrating species or its configuration. Resistivity measurements effectively indicate the number of Frenkel defects removed from

the lattice, but not the mechanism.

Lattice parameter measurements can be combined with resistivity measurements to give a more detailed picture of the defect structure. The advantage of lattice parameter measurements was pointed out in 1954 by Tucker and Sampson,³ who concluded that, since the effect of interstitials should be nearly an order of magnitude greater than that of vacancies, the changes in lattice parameter would reveal the interstitial concentration.

As in the case of electrical resistivity measurements, lattice parameter measurements alone cannot distinguish the migrating species, since most of the recovery is by interstitial-vacancy annihilation. However, if long-range migration of one type of defect takes place, a fraction of the migrating defects can reach other sinks (such as dislocations or surfaces). The nature of the migrating defect can therefore be determined unambiguously by measuring the annealing of defects that do *not* anneal by annihilation; this small effect can be detected by close comparison of electrical resistivity and lattice parameter changes.

The first measurements of irradiation-induced lattice expansion of copper were made by Simmons and Baluffi,⁴ who investigated deuteron-irradiated copper foils. The thermal recovery of the expansion was measured during warming to 90°K (by correcting for thermal expansion). The results were compared to the resistivity measurements of Cooper, Koehler, and Marx,⁵ and it was concluded that the ratio $\Delta\rho/(\Delta a/a)$ is approximately constant (and equal to $700\ \mu\Omega\text{cm}$, to about 20%) throughout all stages of damage and thermal recovery, including data taken at 227 and 302°K. However, the sensitivity was limited by the fact that both the ir-

radiation and the annealing of the specimens in the two experiments differed significantly. Further, the error in lattice parameter measurements was about 10 ppm (i. e., $\pm 3.6 \times 10^{-5} \text{ \AA}$), or about 4% of the total damage. Because of these limitations, the question of whether the annealing mechanisms involved close-pair recombination, interstitial migration, vacancy migration, or other processes could not be resolved.

More recent lattice parameter measurements have been made on neutron-irradiated single crystals of copper by Himmler *et al.*⁶ These measurements were made at 4.2 °K after 10-min isochronal anneals. Comparison to electrical resistivity measurements led to the conclusion that there was a difference in the relative height of the annealing stages for the two properties. It was argued that this difference in height was a result of annihilation in the different stages of defects that differ in specific resistivity and/or volume change. As in the previous work, however, the results suffered in detail from lack of precision in the lattice parameter measurements (the error was given as $\pm 5\%$ of the measured change, or on the order of 15-ppm error in the determination of the lattice parameter) and from the fact that the resistivity specimens were not irradiated and annealed simultaneously with the lattice parameter specimen (although in one case the resistivity damage was measured simultaneously with the lattice parameter specimen irradiation).

The present experiment was begun at about the same time as the work of Himmler *et al.*, but differs in two major respects: First, it was designed to incorporate a separate specimen for simultaneous measurements of electrical resistivity, thereby providing a means of comparing results for specimens having both irradiation and annealing histories as nearly identical as possible. Second, the lattice parameter measurements were made by the Bond method,⁷ using a high-precision Compton spectrometer,⁸ with a resultant limit of error on the order of 1 ppm in the lattice parameter determination. With this high precision, details can be resolved that have not been observable in the earlier work.

II. EXPERIMENTAL PROCEDURE

Neutron irradiation has the advantage that measurements can be made of the lattice parameter change of a large crystal, since the damage is fairly uniform throughout the crystal. Problems associated with bending or buckling of foils are thus eliminated. A new experimental difficulty is added, however, since measurements of the lattice parameter cannot be made in the reactor environment. The neutron irradiation at 4.2 °K must be followed

by transfer of the samples to the measuring facility without permitting the temperature to rise.

The general approach in this experiment has been to irradiate a capsule that is a demountable component of the helium chamber in the measuring cryostat. This capsule, in the form of a double-walled stainless-steel Dewar, contains the copper single crystal, a copper wire resistivity specimen, thermocouples, a carbon resistor, and heaters for temperature measurement and control (see Fig. 1). The instrumentation leads pass through the top (through the liquid-helium chamber), and the single crystal is enclosed in the vacuum chamber at the bottom.

The crystal cover, which completes the vacuum chamber of the capsule, can be removed in the cryostat under vacuum, so that the capsule can be irradiated, transferred to the cryostat, and the crystal exposed to the x-ray beam without warm up above 4.2 °K. A detailed description of the capsule, associated equipment, and transfer procedure has been given previously.⁹ The important factor for the purpose of this experiment is that the resistivity specimen and the single crystal are mounted with good thermal contact in a space that is less than 5 cm high by 1 cm in diam, so that the irradiation and isochronal annealing histories of the two specimens are as nearly identical as possible.

The single crystals used in these experiments were high-purity low-dislocation-density crystals obtained from Oak Ridge National Laboratory.¹⁰

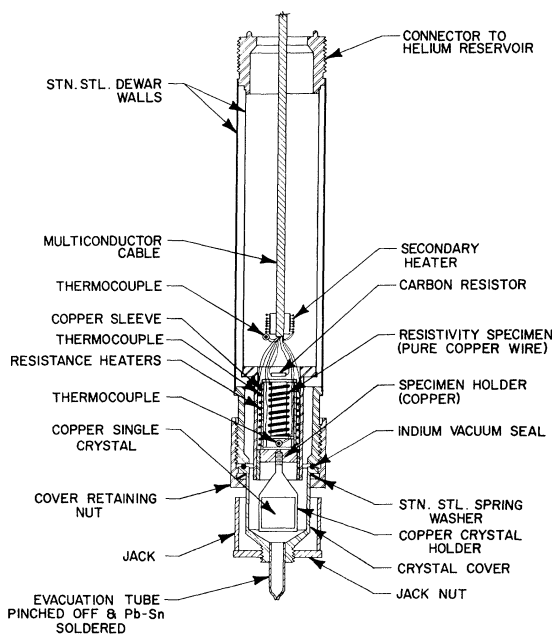


FIG. 1. Cross section of the irradiation cryocapsule.

However, the mounting procedure used was to sinter the crystals with fine high-purity copper powder to a copper support by annealing at 900 °C in vacuum for 24 h. This anneal resulted in an increase in the dislocation density to about 10^6 dislocations per cm^2 . The wire resistivity specimens were drawn from high-purity American Smelting and Refining Co. copper.¹¹ They were encased in Refrasil fiber-glass sleeving, wound on the copper core, and then annealed at 700 °K for 1 h in vacuum. Resistivity ratios (20 °C–4.2 °K) were generally greater than 1000, although in one case (run 9) the ratio was only 850.

The irradiations were carried out in the Argonne CP5 liquid-helium facility, Hole VT-53, which included a uranium converter and a boron carbide thermal-neutron absorber.¹² The resulting fission spectrum had a flux of 7×10^{11} neutrons per cm^2 per sec with energy greater than 0.5 MeV, with only about 10^8 thermal neutrons. The nominal irradiation times were 2 weeks for each irradiation, which resulted in a total dose of $\sim 8 \times 10^{17}$ neutrons per $\text{cm}^2 > 0.5$ MeV. It was possible to monitor the increase in resistivity during irradiation, and the total induced resistivity could be compared to the resistivity measured after transfer to the cryostat to verify that no annealing had taken place during the transfer.

The resistivity measurements were made with the same techniques and essentially the same equipment described earlier.^{11,13} Some improvement may have resulted from the greater length of the resistivity specimens (~ 20 cm, compared to 7 cm in the earlier work) and from the fact that the sample temperature should have been quite uniform during the anneals because of the heater arrangements. The resulting resistivity measurements were much more accurate than the lattice parameter measurements.

The limitation of accuracy in this experiment, as in the earlier x-ray work,^{4,6} is in the lattice parameter measurements. These measurements were made by the Bond method,⁷ which involves measurement of a characteristic reflection on both sides of the incident beam and calculation of the lattice parameter from the difference in the crystal position. A number of factors must be considered to obtain high accuracy,^{7,9,14} and these factors were optimized as much as practicable in view of the special nature of the experimental requirements (i. e., high radioactive background and measurements at 4.2 °K).

One of the most significant advantages in this experiment was the opportunity to use a Compton spectrometer⁸ loaned by the University of Chicago. It was possible with this equipment to measure the lattice parameter with a precision on the order of

1 ppm. The lattice parameter measurements were not corrected for constant sources of error, such as axial divergence or refraction, because the experiment was concerned only with changes in the lattice parameter, not the absolute value.

The lattice parameter was measured by determining the angular positions corresponding to the (400) reflection of the $K\alpha_1$ characteristic wavelength of the cobalt x-ray beam. Details of the procedure have been reported previously.^{9,14} The angular positions were determined by counting for 10 sec at a given angle, increasing the angle by a fixed increment of 15" of arc, and repeating until the high-intensity portion of the peak had been mapped. The data were analyzed with a digital computer by two techniques as shown in Fig. 2.

First, the midchord angles were determined for each point on the ascending side of the peak, and a least-squares line was drawn through the points and extrapolated to the peak maximum. For uniformity only the region from 80 to 98% of the peak was used for the least-square analysis. The top 2% of the peak was not used because of the significance of the background and electronic noise in that region. The standard deviation of the least-squares analysis was usually less than 1" of arc, which would correspond to about 0.4-ppm error in the lattice parameter.

Second, the peaks were analyzed by plotting the derivatives of the peak for the top 5%. A least-squares analysis was used to determine the angular position corresponding to zero slope. This procedure is equivalent to fitting a parabola to the peak maximum. The standard deviation in this analysis was on the order of 20" of arc in most cases, but comparison to the first method usually gave lattice

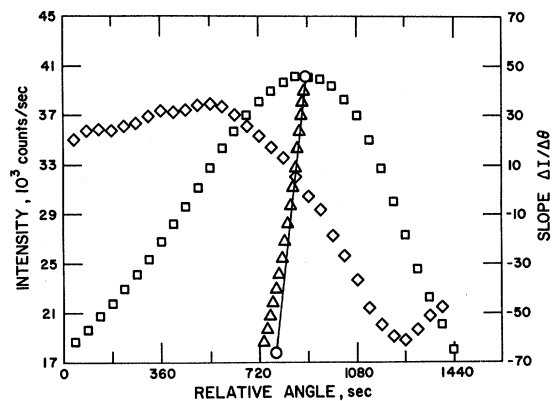


FIG. 2. Illustration of the methods used to calculate the angle associated with a diffraction peak; \square : measured intensity, \diamond : calculated slope, Δ : calculated midchords, \circ : endpoints of the least-squares line through the midchords in the range (0.80–0.98) I_{max} .

parameter that were about 1 ppm smaller. The difference results from the slight skewness of the peak, which is shown by the midchord line in Fig. 2. It appears that either analysis should give good results; the first is slightly more accurate, however, because it includes data from a larger portion of the peak, and was the method used to obtain the results discussed in this paper. The second method was used only as a check on the first; a significant difference occasionally led to detection of a card-punching error that might otherwise have been overlooked.

The lattice parameter was determined as an average of several measurements. The number of averaged measurements was two in run 5, three in run 8, and four in run 9. The number of measurements before and after irradiation and after the high-temperature anneal was usually greater. The total spread in the measurements of $\Delta a/a_0$ after a particular anneal was generally less than 2 ppm, although in a few cases the spread was 3 ppm or greater; the average spread for the 49 anneals in run 9 was 2.1 ppm. The standard deviation was calculated for the data of run 9 for two cases; for eight measurements after irradiation and thirteen measurements after the 675 °K anneal the results were $\sigma = 1.6$ and 1.7 ppm. For run 9, where most results represent an average of four measurements, the standard error of the mean is therefore less than 1 ppm.

The measurements were made at 4.2 °K before and after irradiation and after isochronal anneals to temperatures from 35 °K to 675 °K. The capsule used in run 5 was assembled with soft solder, so that the maximum annealing temperature was 440 °K. The capsule was modified for the later runs to permit annealing to 675 °K, which makes possible almost complete recovery of the electrical resistivity and lattice parameter damage.

Temperature control at low temperatures was a problem, because it was necessary to boil off all the liquid helium, heat to the desired temperature, then cool by transferring liquid helium. In both runs 5 and 8, the first anneal resulted in a brief temperature pulse sufficiently high that no further annealing of the resistivity specimens occurred below 70 or 80 °K. The isochronal annealing times were 5 min in run 5 and 10 min in run 8. In run 9, no such pulse occurred; the first anneal was at 35 °K for only about 2 min, then 5-min anneals were used to 65 °K, and 10-min anneals at all other temperatures through 675 °K. Although the brevity of the pulses allowed some lattice parameter data to be obtained for temperatures down to about 35 °K for run 5 and 50 °K for run 8, because the crystal does not heat as rapidly as the resistivity specimen, these data will not be included because of the lack

of corresponding resistivity data.

III. EXPERIMENTAL RESULTS

The resistivity recovery data for runs 5, 8, and 9 are shown in Fig. 3. The straight-line segments connect the data points measured in run 9. Although minor differences are apparent from run to run, the recovery is similar in all three cases. The corresponding lattice parameter recovery data are plotted in Fig. 4, with the run-9 resistivity recovery shown by the solid line for comparison. Again, there are minor differences in the recovery behavior from run to run. In addition, comparison of the recoveries of the two properties reveals differences that are relatively small, but consistent and significant.

It should be emphasized that it is not sufficient to compare the data directly in this way: The small differences in the annealing behavior from run to run are nearly as great as the differences in annealing of the two properties. This experiment was designed to eliminate the uncertainty because of variations in irradiation or annealing conditions, by direct comparison of the two properties in each run.

This comparison can be made in a number of ways. The simplest is a plot of the residual lattice parameter change as a function of the residual resistivity change. Figure 5 shows such a plot for all of the usable data obtained in this experiment. Run 3 was similar to run 5, except that a great deal of recovery data was lost because of difficulty with the low-temperature vacuum seal. The annealing temperatures indicated at the top of the figure are approximate, because there are slight differences in the resistivity recovery as a function of temperature for the different runs.

The major source of error in the lattice parameter data is the angle of tilt of the crystal normal from the horizontal plane. This tilt error is particularly significant when the crystal is removed from the cryostat and replaced after irradiation; if the tilt angles are not identical, the total induced change in lattice parameter cannot be measured.

A detailed analysis of the tilt error has been reported recently.¹⁴ This analysis was used to measure the tilt during the annealing in run 8 and to correct the data. In run 9, the crystal was positioned accurately for minimum tilt error, and no corrections were necessary. However, in runs 3 and 5, it was necessary to estimate the total change in lattice parameter (by comparison to run 9) in order to normalize the data plotted in Fig. 5. Except for error due to incorrect normalizing (which may be more important for run 3 because of the limited data range), the standard deviation of the data should be on the order of the radius of the

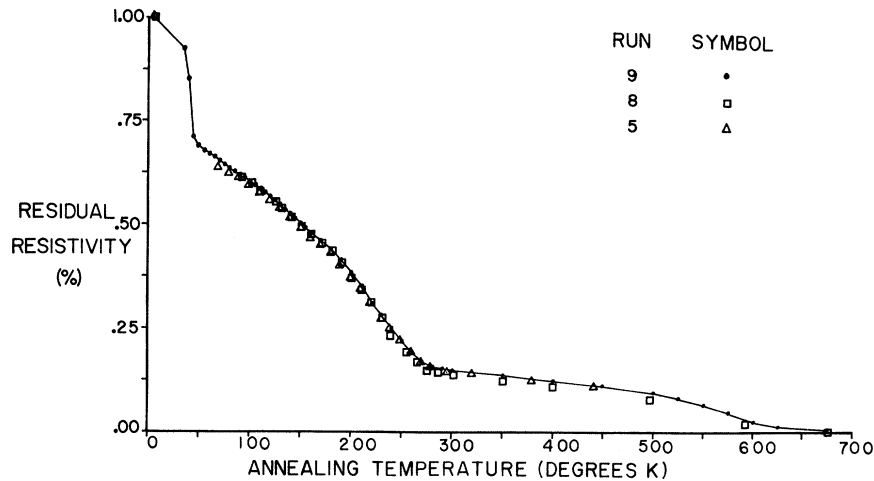


FIG. 3. Residual resistivity recovery. The solid line connects the run-9 data points. The total changes were 9.2 , 8.4 , and $7.5 \times 10^{-8} \Omega \text{cm}$, respectively, for runs 9, 8, and 5.

plotted symbols (or less than 1% of the total damage).

The deviations from the straight line appear to be reproducible from run to run. Run 9 shows the one-to-one recovery expected in stage I (below 50°K); above 100°K the lattice parameter begins to recover more rapidly, as the data drop below the line; then the lattice parameter recovers more slowly to 200°K , shown by the return to the line; and in the range below 300°K there is a deviation above the line, indicating a slower lattice parameter recovery. The recovery of both properties is essentially complete after the high-temperature anneals.

The significance of these results will be discussed in Sec. IV. It must be noted that the simple manner used to present the data in Fig. 5 has its limitations. The deviations are not as evident as they could be because the vertical scale is set by

the total damage. Further, the temperature is not shown as clearly as might be desired. Plots of damage ratios as a function of temperature overcome these difficulties to some extent; however, it seems more desirable to first develop a simple model, then plot the results in a way that shows the conclusions that can be based on the model. This procedure will be followed in Sec. IV.

IV. DISCUSSION OF RESULTS

The simplest model of the damaged crystal is that in which the damage is assumed to be related directly to the density of vacancies and interstitials. This model will be referred to as the linear superposition model, since it is based on the approximation that the effects on the lattice parameter and on the electrical resistivity can be represented as a linear superposition of the effects due to single isolated vacancies and interstitials.

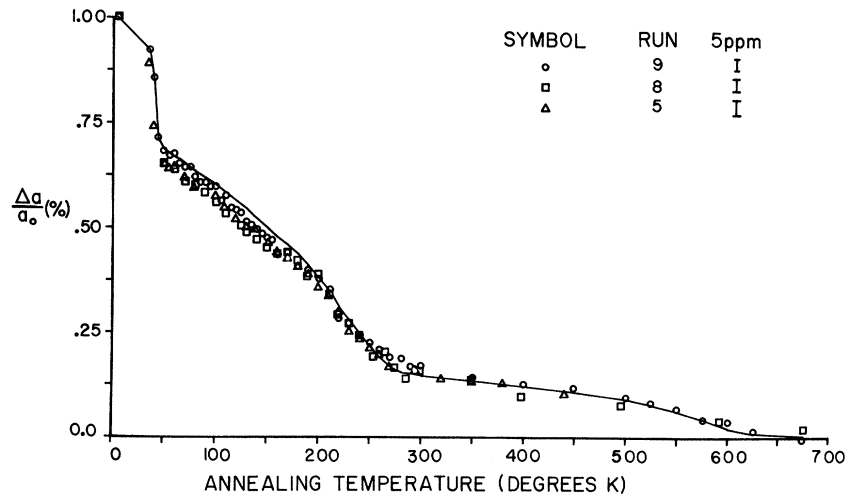


FIG. 4. Lattice parameter recovery. The solid line shows the run-9 resistivity recovery for comparison. The 5-ppm error bars are shown in the key for different runs. The total changes were 152, 139, and 130 ppm, respectively, for runs 9, 8, and 5.

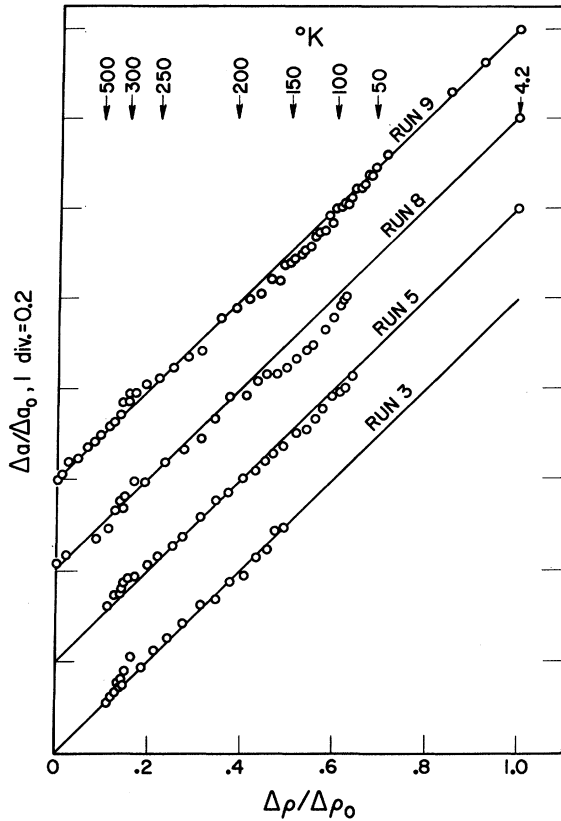


FIG. 5. Lattice parameter recovery as a function of resistivity recovery. The vertical scale is 20% per division.

This model permits a simple analytical expression of the radiation damage in the form

$$\Delta\rho = \rho_i n_i + \rho_v n_v, \quad (1)$$

where $\Delta\rho$ is the increase in electrical resistivity, ρ_i and ρ_v are the specific resistivities ($\mu\Omega$ cm per unit concentration of isolated interstitials and vacancies, respectively), and n_i and n_v represent the concentrations of defects.

A similar expression can be written for the lattice parameter increase

$$\Delta a/a_0 = \alpha_i n_i + \alpha_v n_v, \quad (2)$$

where α_i , α_v are the fractional changes in lattice parameter per unit concentration of interstitials and vacancies, respectively. It is convenient to define the ratios of the damage parameters, which are assumed constant, as

$$k_r = \rho_v/\rho_i \quad (3)$$

and

$$k_a = -\alpha_v/\alpha_i. \quad (4)$$

Equations (1) and (2) can then be solved readily to obtain the following expressions for the vacancy and interstitial concentrations in terms of the measured damage,

$$n_v = \frac{\Delta\rho/\rho_i - (\Delta a/a_0)/\alpha_i}{k_a + k_r}, \quad (5)$$

$$n_i = \frac{k_a \Delta\rho/\rho_i + k_r (\Delta a/a_0)/\alpha_i}{k_a + k_r}. \quad (6)$$

Because of the small differences, it is useful to have a direct measure of the difference in concentrations, relative to the total concentration of defects. This ratio is given from Eqs. (5) and (6) by

$$\frac{n_v - n_i}{n_v + n_i} = \frac{(1 - k_a) \Delta\rho/\rho_i - (1 + k_r) (\Delta a/a_0)/\alpha_i}{(1 + k_a) \Delta\rho/\rho_i - (1 - k_r) (\Delta a/a_0)/\alpha_i}. \quad (7)$$

Before these relations can be evaluated from the data, values must be assumed for the constants.

A reasonable approximation for the resistivity is $\rho_i = \rho_v = 150 \mu\Omega$ cm per unit concentration; that is, the resistivity of a Frenkel defect is taken as $3 \mu\Omega$ cm/at.%, and the resistivities of vacancies and interstitials are assumed equal.

Calculations of the effects of point defects on the lattice parameter have been reported by Tucker and Sampson,³ who reported for copper $\alpha_i = 1.0$ and $\alpha_v = -0.2$.

The recovery data for run 9 have been used to calculate the vacancy and interstitial concentrations as a function of temperature; the results are plotted in Fig. 6. This particular choice of constants leads to the result that the vacancy concentration exceeds the interstitial concentration throughout the range; while this is not impossible, it is unlikely that the direct consequence, that vacancies are removed faster in all stages than interstitials, is true. In particular, it is expected that the numbers of vacancies and interstitials annealing in stage I are equal.

If the value of α_v is changed to -0.5 , the concentrations following irradiation are essentially equal; further they remain equal through stage-I annealing, as shown in Fig. 7. A brief scrutiny of Fig. 7 also shows that the recovery of interstitials is slightly faster than that of vacancies in the first part of stage II, but then becomes slower until stage III is essentially complete, and that the recoveries above about 350°K are nearly equal. These differences in recoveries are small, however, and difficult to distinguish clearly in this plot.

A more useful plot of all of the data is given in Fig. 8, which shows the excess vacancy fraction, calculated from Eq. 7, as a function of temperature. The significance level of the data is indicated by the 1-ppm error bars plotted along the tempera-

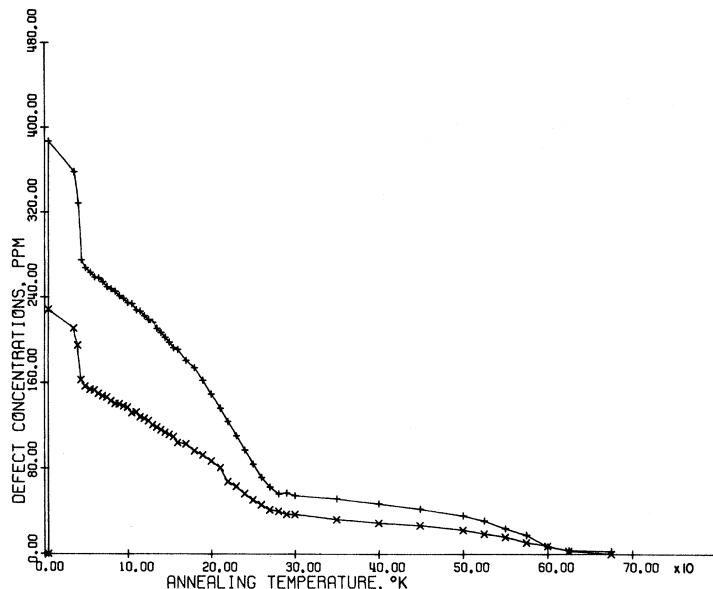


FIG. 6. Calculated vacancy (+) and interstitial concentration (x) as a function of annealing temperature for run 9, assuming $\alpha_i = 1$, $\alpha_v = -0.2$.

ture axis. The zero level for each run is indicated by a horizontal line. The discrepancies between the data and the zero lines for runs 3 and 5 are caused by a lack of accurate data concerning the total lattice parameter change. However, the curve shape is insensitive to this normalizing value; in fact, it is not very sensitive to the values of the constants used in Eq. (7). If the values in Fig. 6 were used in this plot, the only changes would be a vertical shift and a 25% increase in the vertical scale.

Other values of the constants α_i and α_v were also considered. It can be shown from Eqs. (1) and (2)

that the assumption $n_i = n_v$ leads to the result

$$\frac{\Delta \rho}{a/a_0} = \frac{\rho_i + \rho_v}{\alpha_i + \alpha_v} . \quad (8)$$

The experimentally determined value of this ratio was $605 \mu\Omega \text{ cm} (\pm 2\%)$. Therefore, for the assumed resistivity of a Frenkel defect ($3 \mu\Omega \text{ cm/at. } \%$), the sum $\alpha_i + \alpha_v \approx 0.5$. A range of values satisfying this relation was used, with α_i varying for 0.6–2.0. There were no observed differences in the plotted results except in over-all magnitude; the shapes of the curves plotted in Fig. 8 are independent of the choice of parameters within the stated limits.

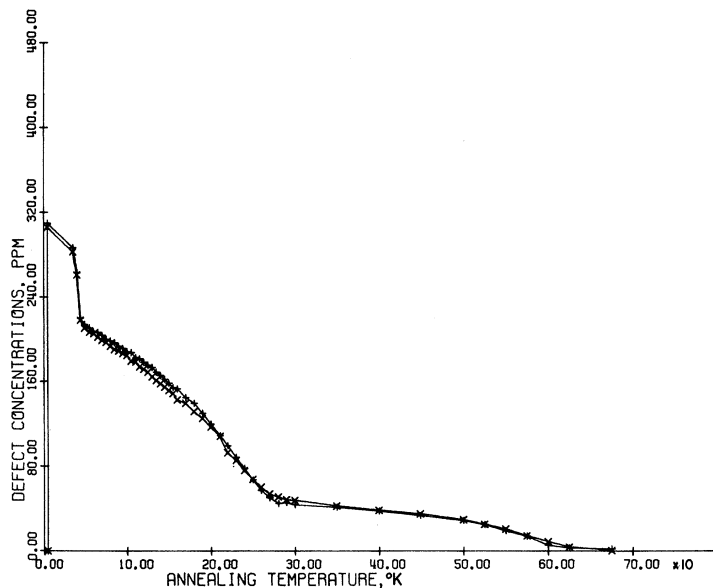


FIG. 7. Calculated vacancy (+) and interstitial concentrations (x) as a function of annealing temperature for run 9, assuming $\alpha_i = 1.0$, $\alpha_v = -0.5$.

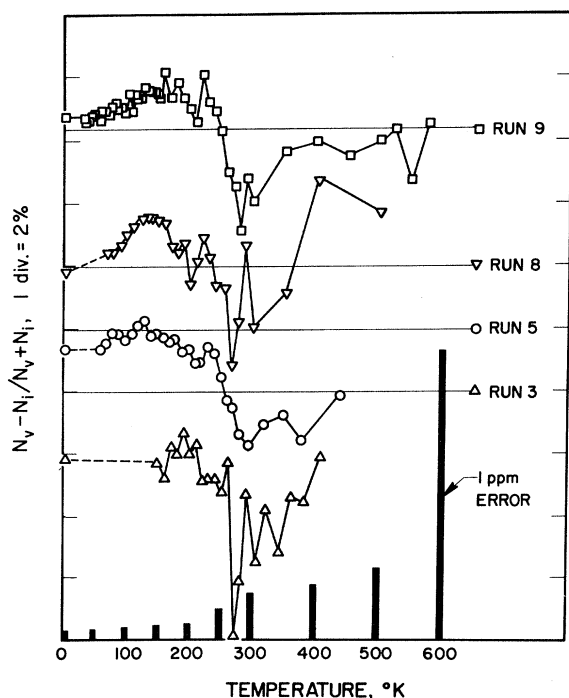


FIG. 8. Calculated excess-vacancy fractions for runs 3, 5, 8, and 9, with $\alpha_i = 1.0$, $\alpha_v = -0.5$. The error bars indicate the significance of an error of 1 ppm in the measured lattice parameter at various temperatures (calculated for run 9).

The results of run 3 are included only for completeness, and to show the general agreement with the later, more accurate, data. Note that above about 330 °K, the deviations from the zero line are only of the order of the 1-ppm error bar, and are not considered significant.

There are three dominant features exhibited by the data in this figure. First, there is no significant deviation from equal numbers of vacancies and interstitials in stage I. This observation is in agreement with the generally accepted interpretation that stage I recovery is primarily a result of correlated vacancy-interstitial recombination.

Second, the excess-vacancy fraction begins to increase at temperatures below 100 °K, reaching a maximum of slightly less than 2% near 150 °K. Again, this observation is consistent with earlier observations^{2,15} that interstitials become mobile, undergoing long-range migration, at temperatures at the high end of stage I. The implication is that interstitials are migrating freely throughout this temperature range; as the concentration of vacancies decreases, a larger fraction of the interstitials reach other sinks (surfaces or dislocations, for example). These sinks will be referred to as "secondary sinks" to distinguish them from the

primary sinks associated with vacancy-interstitial annihilation. Since the stage I recovery is about 30%, and the recovery at 150 °K is about 50%, about 21% of the original interstitials have been annealed out, along with about 20% of the original vacancies. In other words, about 5% of the interstitials annealing out in this temperature range have not recombined with vacancies; they have migrated to secondary sinks.

Finally, in the range 150–280 °K, the recovery shows a complicated behavior but a definite decrease in excess vacancy concentration. The obvious conclusion is that, if vacancies migrate at any temperature, it is in this range. The most dramatic feature in this range is the continuous reduction in excess-vacancy concentration shown from 220 to 280 °K. This reduction is very sharply defined and accurately reproduced in runs 5, 8, and 9. The total recovery in this range is about 15%, but the excess-vacancy fraction decreases from about +1% to about -3 or -4%. Thus while the total recovery in this range is about 15%, about 1% of the original vacancy concentration is annealed out at secondary sinks. The conclusion from this model is clear: Vacancies undergo long-range migration in stage III in copper.

There are also some less significant features that should be mentioned in regard to Fig. 8. First, there is a sharp increase in the apparent excess-vacancy fraction in the small temperature range 200–220 °K. This feature is reproduced in runs 5, 8, and 9 to a sufficient degree that it is considered a real effect. Possible sources of this peak are, in terms of the present model, the removal of interstitials or the addition of vacancies. If interstitials are suddenly released from traps or clusters in this range, some of them could migrate to secondary sinks and this result might be expected. The fact that this increase in excess-vacancy concentration follows a decrease should also be considered, for it implies that vacancies are mobile at temperatures down to about 160 °K. These mobile vacancies may be present in the form of divacancies, of course; the present model does not distinguish cluster sizes.

The alternate explanation for the peak, as evidence of an increase in the vacancy concentration, can only be considered by an extension of the model to include clustering effects. For example, the effect could result from a break up of vacancy clusters (including divacancies) if clustering affects the lattice parameter and the resistivity differently. In particular, if divacancies were to become unstable, there is in all probability a unique binding energy associated with the break up into single vacancies. Thus the rather sharp increase in apparent excess-vacancy concentration might be expected

if this process were to occur; in fact, the decrease in excess-vacancy fraction in the lower temperature range would also be expected if the migration energy of a divacancy (or cluster) is less than the binding energy.

It has been assumed in the preceding discussion that the dominant process detected in the comparison of the two properties during annealing is that some small fraction of the migrating defects reach secondary sinks (i. e., sinks other than the opposite type of defect). It has been stated elsewhere^{6,16} that all recovery is due to recombination of interstitials and vacancies, and the variations in the recoveries of the measured properties arise from different defect configurations.

Some quantitative data can be provided to aid further consideration of this interpretation. Table I shows the result given by Himmler *et al.*⁶ for neutron-irradiated copper, along with the results of the present experiments. Variations in the recovery ratios can be noted in the different temperature ranges selected by these workers, and these variations tend to be reproduced in the different experiments. However, a much more dramatic difference in these ratios is observed if the temperature ranges are defined for the different experimental runs in terms of the observed extremes. The results are shown in Table II for the data obtained in these experiments. The ratio R is the ratio of resistivity recovery to lattice parameter recovery in the temperature range indicated in the left-hand column for each run. The last value represents the total recovery from 4.2 °K to the highest annealing temperature; for run 3, this value is only an estimate.

The most complete data are for run 9, which will be used as the basis for this discussion. The remaining data are considered as confirmation of the general features of the annealing spectrum of copper. First, it should be noted that the ratio for 4.2–60 °K is very nearly the same as for 4.2–

TABLE II. Incremental recovery ratios $R = \Delta\rho/(\Delta a/a_0)$ for the temperature ranges defined by the extremes shown in Fig. 8.

Run 9		Run 8		Run 5		Run 3	
T (°K)	R ($\mu\Omega$ cm)	T (°K)	R ($\mu\Omega$ cm)	T (°K)	R ($\mu\Omega$ cm)	T (°K)	R ($\mu\Omega$ cm)
4.2	615	4.2	557	4.2	574	4.2	...
60	494	80	404	60	461	...	513
160	948	124	911	130	719	190	...
211	360	200	402	210	508	...	784
220	996	219	911	230	743	220	711
280	480	265	553	295	394	270	260
675	606	675	604	440	583	405	530
4.2		4.2		4.2		4.2	

675 °K (the last value in the column). Since recovery is essentially complete after the 675 °K anneal, this value is in excellent agreement with the ratio observed for the irradiation damage at 4.2 °K. Thus the recovery in stage I is apparently due to recombination, with the relative properties of the combining defects the same as the average properties of the induced defects. The significance of this ratio in stage I should not be disregarded, for it provides additional support for the assumption of the linear superposition model.

The ratios in the remaining temperature ranges alternate between low and high – below 500 $\mu\Omega$ cm and above 900 $\mu\Omega$ cm. In the interpretation of the above workers,^{6,16} then, there must be at least three configurations of combining defects, and these combine in six different temperature ranges. If the number of configurations is limited to three, then the low-ratio configuration anneals in three separate temperature ranges. These speculations seem unduly complicated in comparison to the linear superposition model, and will not be considered further.

One further possibility that must be considered is the effect of defect clustering. Since the defects are certainly not produced as a random distribution of isolated defects, the influence of clustering should not be ignored. The difficulty in interpreting the observed effects in terms of clustering arises from the lack of theoretical information concerning the effect of clustering on the properties of the material. In the absence of such information, it has simply been assumed in the linear superposition model that there is no effect (or at least that the effects is unchanged).

In general, however, clustering could conceivably lead to the observed deviations. The possibility that the positive slope in the curves of Fig. 8 in the

TABLE I. Incremental recovery ratios $R = \Delta\rho/(\Delta a/a_0)\mu\Omega$ cm) for the temperature ranges reported by Himmler *et al.*

T (°K)	Himmler <i>et al.</i>		run 5	Present work	
	run I	run II		run 8	run 9
4.2					
60	373	408	575	591	587
300	506	570	610	620	663
670	515	538	...	582	495
4.2	457	506	583	604	606

range of 200–220 °K can be attributed to divacancy break up has already been discussed. Similarly, other aspects of the annealing curves could be attributed to interstitial or vacancy cluster formation or dissolution. Such an analysis at the present time, however, would be based entirely on speculation.

V. CONCLUSIONS

It has been shown that, by comparison of the simultaneous recovery of the lattice parameter and electrical resistivity induced by low-temperature neutron-irradiation of copper, significant and reproducible variations occur in the ratio of the recoveries of the two properties.

These variations can be explained by considering that the migrating species has a finite probability of removal at sinks other than defects of the opposite type. This explanation leads to the following conclusions:

- (a) Stage-I annealing is primarily due to recombination of vacancies and interstitials.
- (b) Interstitials become mobile at relatively low temperatures and are the migrating species to about 160 °K.
- (c) The recovery above 160 °K appears to be dominated by vacancy migration; the migrating species may be the divacancy. Stage-II recovery, in gen-

eral, is quite complex.

(d) The most pronounced deviation observed is in the range 220–280 °K, where the migrating species is in all probability the single vacancy. This behavior in stage III appears to be quite uniform and uncomplicated.

(e) There appears to be no advantage or justification in attempting to describe the data in terms of various defects configurations. However, more complex explanations in terms of clustering effects may be possible.

ACKNOWLEDGMENTS

This paper would not be complete without a statement of our gratitude to Dr. B. D. Sharma, presently at Trombay, Bombay, India, for his efforts in the initial stages of this experiment. Our thanks are also extended to Dr. C. S. Barrett and the University of Chicago for the extended loan of the high-precision Compton spectrometer, to the members of the Metallurgy Design Group and Janis Research Corp. for the design and construction of the special-purpose cryostat, and to Dr. L. Guttman of the Solid State Science Division, ANL, for helpful discussions. This work was performed under the auspices of the U. S. Atomic Energy Commission.

¹See for example, T. H. Blewitt, *Radiation Damage in Solids, Proceedings of the International School of Physics, "Enrico Fermi", Course XVIII*, edited by D. S. Billington (Academic, New York, 1962), pp. 630–716.

²J. W. Corbett, in *Solid State Physics, Suppl. 7* (Academic, New York, 1966).

³C. W. Tucker and J. B. Sampson, *Acta. Met.* **2**, 433 (1954).

⁴R. O. Simmons and R. W. Baluffi, *Phys. Rev.* **109**, 1142 (1958).

⁵H. G. Cooper, J. S. Koehler, and J. W. Marx, *Phys. Rev.* **97**, 599 (1955).

⁶U. Himmler, H. Peisl, A. Sepp, W. Waidelich, and H. Wenzl, *Phys. Rev. Letters* **19**, 956 (1967).

⁷W. L. Bond, *Acta Cryst.* **13**, 814 (1960).

⁸A. H. Compton, *Rev. Sci. Instr.* **2**, 365 (1931).

⁹E. E. Gruber, T. H. Blewitt, J. A. Tesk, B. D. Sharma, and R. E. Black, *Rev. Sci. Instr.* **40**, 1429 (1969).

¹⁰R. W. Young, Jr., and J. R. Savage, *J. Appl. Phys.* **35**, 1917 (1964).

¹¹J. A. Horak, ANL Report No. 7185, 1966 (unpublished).

¹²A. C. Klank, T. H. Blewitt, T. Scott, and J. Minarik, in *Pure and Applied Cryogenics, Vol. 6: Liquid Helium Technology* (Pergamon, New York, 1966), pp. 373–381.

¹³J. A. Horak, T. H. Blewitt, and M. E. Fine, *J. Appl. Phys.* **39**, 326 (1968).

¹⁴E. E. Gruber and R. E. Black, *J. Appl. Cryst.* (to be published).

¹⁵D. O. Thompson, T. H. Blewitt, and D. K. Holmes, *J. Appl. Phys.* **28**, 742 (1957).

¹⁶H. Peisl and W. Waidelich, in *The Interaction of Radiation with Solids, Proceedings of the Cairo Solid State Conference at the American University at Cairo, Egypt*, 1966, edited by A. Bishay (Plenum, New York, 1967), p. 489.